



Damage mechanism in AlSi1MgMn alloy

G. Mrówka-Nowotnik *

Department of Materials Science, Rzeszow University of Technology,
ul. W. Pola 2, 35-959 Rzeszów, Poland

* Corresponding author: E-mail address: mrowka@prz.edu.pl

Received 10.12.2007; published in revised form 01.02.2008

ABSTRACT

Purpose: The main task of this work was to study the fracture mechanism in 6082 aluminium alloy.

Design/methodology/approach: Microstructure and fractographic examination has been carried out on the samples in the peak aged condition after static tensile tests, crack resistance test and tensile test in the presence of sharp notch using an optical microscope - Nikon 300, scanning electron microscope HITACHI S-3400 (SEM) in a conventional back-scattered electron mode and JEOL - JEM 2100 ARP TEM/STEM electron microscope on polished sections etched in Keller solution.

Findings: It has been found that, at room temperature, general cavitation (nucleation of voids) occurs after appreciable strain. The nucleation of voids results from debonding along certain particle/matrix interfaces. Observations of microstructure revealed second fracture mechanism initiated by cracking of brittle intermetallic phases.

Practical implications: All this knowledge – identification of the microstructural parameters for the different modes of void nucleation and cracking of intermetallic phases leading to fracture of the alloy – can be used to predict maximum ductility before fracture of tensile specimens.

Originality/value: For deformation at room temperature different void populations have been defined: void nucleated by intermetallic particle fracture, by β particle/matrix decohesion and by α particle/matrix decohesion.

Keywords: Fracture mechanics; Electron microscopy; Microstructure; Intermetallic phases

PROPERTIES

1. Introduction

Aluminium alloys have been widely used since the early 20 century for structural engineering applications, in transportation - aircraft and automotive industries and in civil engineering. Nowadays, new aluminium alloys are further developed to satisfy the demands of the transportation industries for high strength, improved damage resistance as well as reduction of production cost. Heat-treated aluminium alloys of 6xxx series have been developed in order to fulfill these requirements [1-3]. The group of these alloys contains magnesium and silicon as major addition elements and belongs to the commercial aluminum alloys, in which relative volume, chemical composition and morphology of structural constituents exert significant influence on their useful properties [2-6].

Aluminium alloys 6xxx contain a large amount of various intermetallic particles with size typically ranging between 1 to 10 micrometers. Generally, two populations of large particles and

dispersoids can be observed in microstructure of all Al alloys of 6xxx series [5-8]. The large particles consist of an intermetallic phase Mg_2Si or Fe-rich and contain Al, Fe, Mn, Si. The most typical are the plate-like $\beta-Al_3FeSi$ particles and the spherical of $\alpha-Al_{12}(Fe,Mn)_3Si$. The α -phase (Fe-rich coarse particles) is arranged in interdendritic channels and small dispersoids. The brittle, monoclinic $\beta-Al_3FeSi$ phase, which is insoluble during solution heat treatment, is associated to reduced workability and cause a poor surface finish [7-12].

As reported in the literatures [7-10], damage during extrusion initiates by decohesion or fracture of these inclusions. The resistance to damage and fracture depends thus directly on the nature, shape, distribution and volume fraction of the second phase particles. High damage localization has been observed around the coarse particles [7-15]. These particles can either fracture or debond from the matrix, depending on their size, morphology, etc. For this reason, these coarse particles are assumed to be nucleation sites for cracks. The two families of

particles, α and β , give rise to damage, with different void nucleation mechanisms. The damage evolution consists thus in the nucleation, growth and coalescence of different populations of voids. The damage evolution also directly depends on the strength, strain hardening capacity and strain rate sensitivity of the matrix surrounding the voids [7-13].

Microstructure and fracture observation of the samples in the peak aged condition after static tensile tests, crack resistance tests and tensile test in the presence of sharp notch R_m^k allow to define two damage mechanisms. The first one is characterized by nucleation of voids that results from debonding along certain particle/matrix interfaces and the second fracture mechanism was initiated by cracking of brittle intermetallic phases.

2. Material and experimental

This study was performed on the commercial AlSi1MgMn (6082) aluminum alloy (Table 1).

Table 1.
Chemical composition of the investigated alloys, %wt

Alloy	Si	Fe	Cu	Mn	Mg	Cr	Zn	Others	Al
6082	1.2	0.33	0.08	0.50	0.78	0.14	0.05	0.15	bal

The effect of artificial aging on the microstructure, mechanical properties and fracture toughness was presented in previous works [2,3,12]. In this study microstructure and fracture observation were conducted to obtain information about fracture mechanism in investigated AlSi1MgMn alloy.

Microstructure and fractographic examination has been carried out on the samples in the peak aged condition after a) static tensile tests, b) crack resistance tests and c) tensile test in the presence of sharp notch R_m^k . The microstructure of examined alloy was observed using an optical microscope - Nikon 300 on polished sections etched in Keller solution (0.5 % HF in 50ml H₂O). Fracture surface observation was also made in the scanning electron microscope HITACHI S-3400 (SEM), operating at 6-10 kV in a conventional back-scattered electron mode. Chemical composition of the intermetallics was made by EDS attached to the SEM using the software of Thermo Noran. The thin foils were examined in a JEOL - JEM 2100 ARP TEM/STEM operated at 200kV electron microscope. Thin foils for TEM studies were manufactured by cutting 3 mm diameter discs, followed by grinding manually to a thickness of about 0.1 mm. Finally, the disc was thinned electrolytically using a Struers Tenupol jet polishing machine, with a solution (by volume) CH₃OH (84cm³), HClO₄ (3.5cm³) and glycerin (12.5cm³), operating at -10°C and U=28V.

3. Results and discussion

Figure 1 presents fracture surface profile of the specimen of AlSi1MgMn alloy in the peak aged condition after static tensile test. Optical microscope observation showed that the main crack is formed at the interface between matrix and intermetallics

β -Al₃FeSi and precipitates of α -Al(FeMn)Si phases (Fig. 1a). However the secondary cracks occurred in the brittle intermetallic β -Al₃FeSi and α -Al(FeMn)Si phases. The elongated particles aligned along the main loading direction break into several fragments (Fig. 1b).

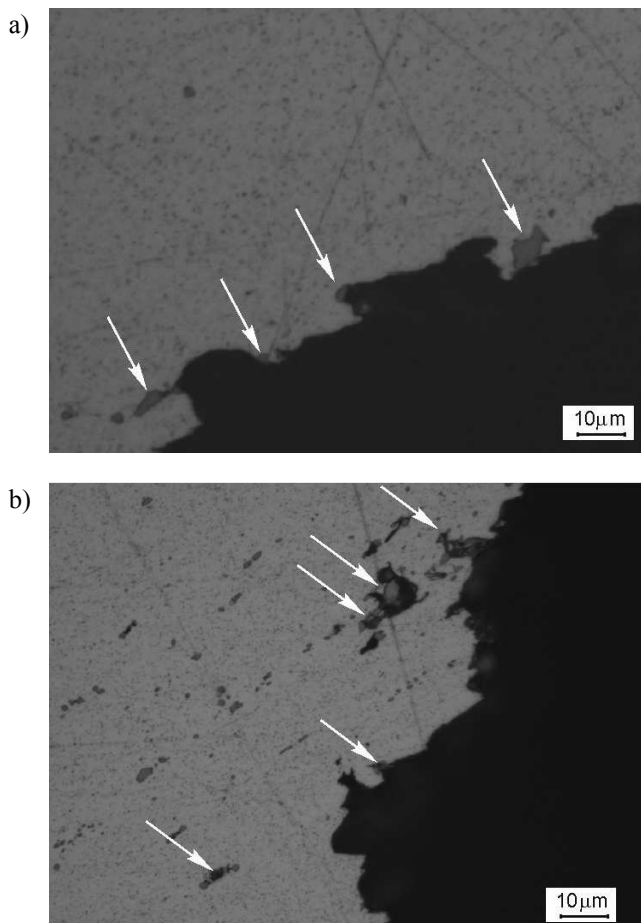


Fig. 1. Fracture profile of specimen after static tensile test. The main crack is formed at the interface between matrix and intermetallics β -Al₃FeSi and precipitates of α -Al(FeMn)Si phases (a) secondary cracks are present in the brittle intermetallic β -Al₃FeSi and α -Al(FeMn)Si phases (matrix/precipitates and cracked α and β intermetallics interface is marked with white arrows in the figures)

TEM observation of microstructure of the aged samples of 6082 alloy with the highest tensile strength in the peak aged condition [12] (Fig. 2) confirmed results of optical microscope observation (Fig. 1). As shown in Figure 2 mechanism of decohesion followed through nucleation of voids at the interface between matrix and intermetallics α -Al(FeMn)Si phase precipitates. SEM observation of fracture, processes in the sample with the highest tensile stress in the presence of sharp notch (Fig. 3), confirmed that fracture initiates within void clusters as a result of a sequence of void nucleation, void growth, and void coalescence.

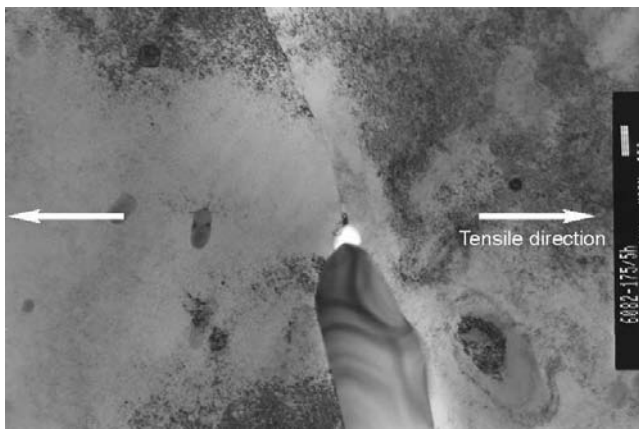


Fig. 2. TEM micrograph of the 6082 alloy subjected to the precipitation hardening process and static tensile test. Visible particle of α -Al(FeMn)Si phases / α -aluminium interface decohesion

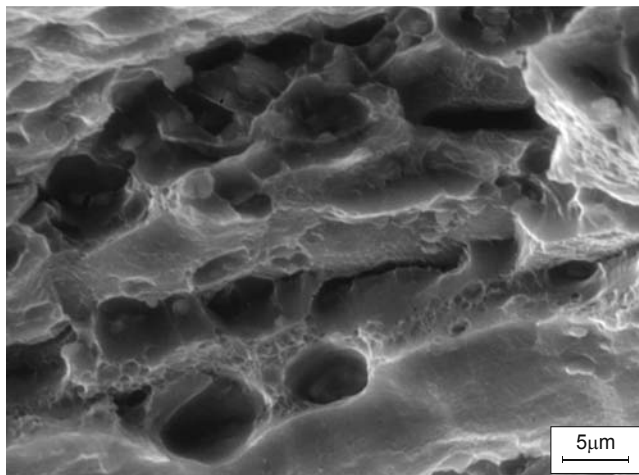


Fig. 3. Fracture surface of the 6082 alloy after static tensile test in the presence of sharp notch R_m^k : a) shear oval dimples formed after coalescence of the linear void sequence b) large dimples around hard intermetallic α (Al₈Fe₂Si) and β (Al₅FeSi) precipitates and smaller around dispersive hardening β -Mg₂Si and α -Al(FeMn)Si precipitates [5,6]

Figure 4 illustrates the change of fracture mode as a function of the particle orientation. The results of SEM observation presents the particles of β -Al₅FeSi [5,6] (Fig. 4a) and Mg₂Si [5,6] (Fig. 4b) phases aligned along the main tensile loading direction break into several fragments. The cracks in the particles are normal to the macroscopic tension axis. The number of fragments increases with increasing particle length. Figure 4 shows also how the fracture mode depends on the particle orientation. It was observed that the majority of the particles oriented in the range of 0° to 45° with to the loading direction lead to particle fractures.

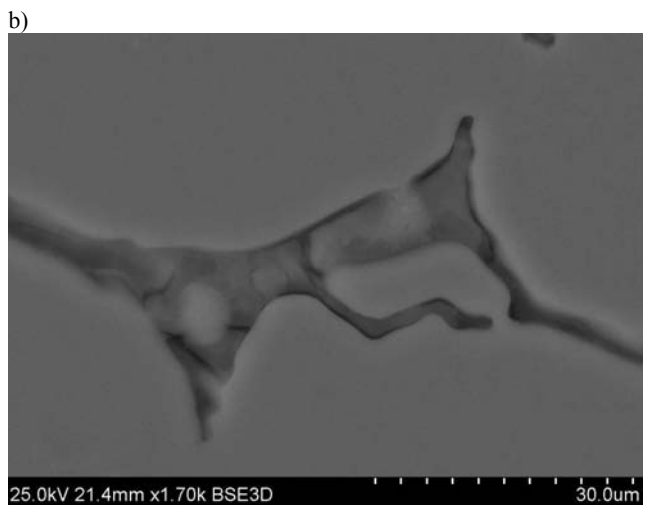
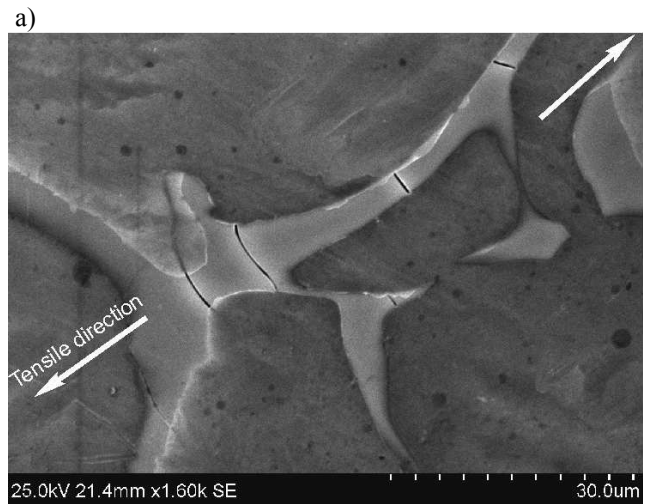


Fig. 4. SEM micrographs of specimens after static tensile test. The main cracks are present in the brittle intermetallic a) β -Al₅FeSi and b) Mg₂Si phases [5,6]

If the particles were oriented in the range of 45° to 90° fracture occurred on particle / α -aluminium interface decohesion (Fig. 2).

Figure 5 presents the fracture in two-phase region of the 6082 alloy after static tensile test in the presence of sharp notch R_m^k . The cell is formed from a deformed matrix band around the cracked α -Al(FeMn)Si particles. The zone of the interface decohesion is present on the interface between interface α -aluminium and α -Al(FeMn)Si particles. In the α -Al(FeMn)Si particles, the numerous cleavage cracks are visible. In the microregion of the solid solution α -Al the oval and open shear dimples are revealed (Fig. 5a). Figure 5b present the microregion of the fracture of mixed morphology. The cleavage facets (α -Al(FeMn)Si) and shear dimples (α -aluminium) are arranged in parallel bands.

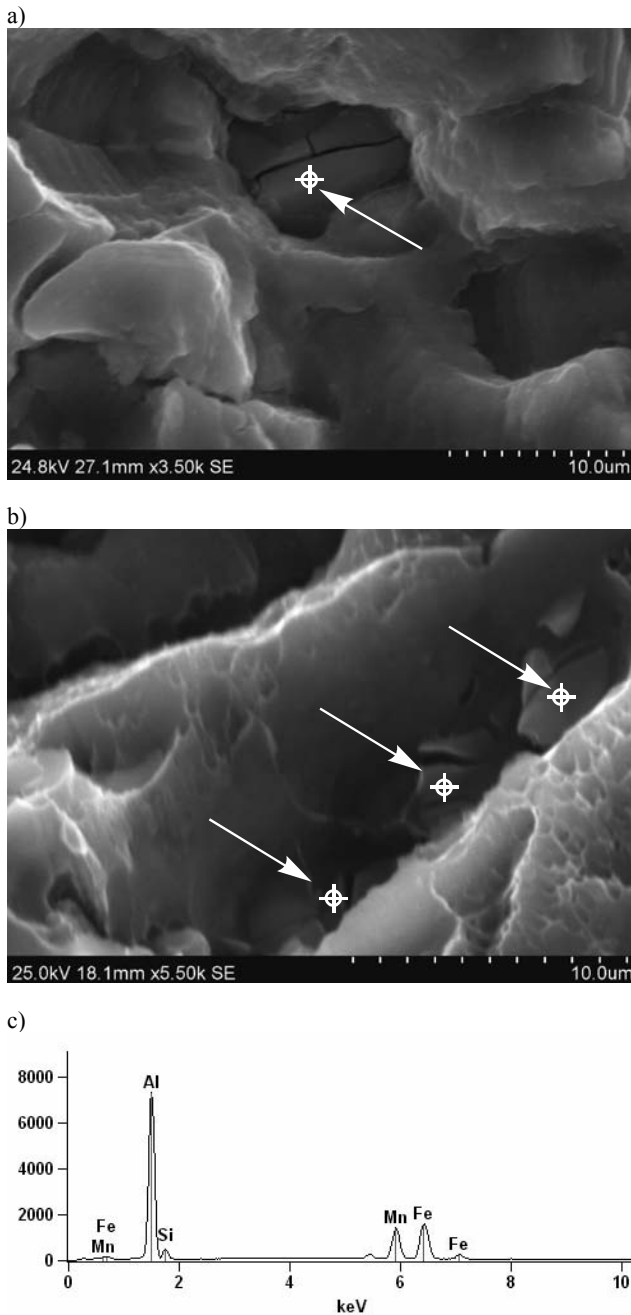


Fig. 5. Fracture in two-phase region of the 6082 alloy after static tensile test in the presence of sharp notch R_m^k (a,b) EDS spectra of cracked α -Al(FeMn)Si particles (points of the EDS analysis are marked with white spots and arrows in the figure)

Acknowledgements

This work was carried out with the financial support of the Ministry of Science and Information Society Technologies under grant No. N507 3828 33.

References

- [1] L.A. Dobrzański, R. Maniara, J.H. Sokółowski, The effect of cast Al-Si-Cu alloy solidification rate on alloy thermal characteristic, *Journal of Achievements in Materials and Manufacturing Engineering* 17 (2006) 217-220.
- [2] G. Mrówka-Nowotnik, J. Sieniawski, Influence of the heat treatment on the microstructure and mechanical properties of 6005 and 6082 aluminium alloys, *Proceedings of the 13th International Conference "Achievements in Mechanical & Materials Engineering" AMME'2005, Gliwice-Wisła, 2005*, 447-450.
- [3] G. Mrówka-Nowotnik, J. Sieniawski, Influence of heat treatment on the microstructure and mechanical properties of 6005 and 6082 aluminium alloys, *Journal of Materials Processing Technology* 162-163 (2005) 367-372.
- [4] L.A. Dobrzański, W. Borek, R. Maniara, Influence of the crystallization condition on Al-Si-Cu casting alloys structure, *Journal of Achievements in Materials and Manufacturing Engineering* 18 (2006) 211-214.
- [5] G. Mrówka-Nowotnik, J. Sieniawski M. Wierzbńska, Analysis of intermetallic particles in AlSi1MgMn aluminium alloys, *Journal of Achievements in Materials and Manufacturing Engineering* 20 (2007) 155-158.
- [6] G. Mrówka-Nowotnik, J. Sieniawski M. Wierzbńska, Intermetallic phase particles in 6082 aluminium alloys, *Archives of Materials Science and Engineering* 28/2 (2007) 69-76.
- [7] D. Lassance, D. Fabrègue, F. Delannay, T. Pardoën, Micromechanics of room and high temperature fracture in 6xxx Al alloys, *Progress in Materials Science* 52 (2007) 62-129.
- [8] S.E. Urreta, F. Louchet, A. Ghilarducci, Fracture behaviour of an Al-Mg-Si alloy, *Materials Science and Engineering A302* (2001) 300-307.
- [9] P. Nègre, D. Steglich, W. Brocks, Crack extension in aluminium welds: a numerical approach using the Gurson-Tvergaard-Needleman model, *Engineering Fracture Mechanics* 71 (2004) 2365-2383.
- [10] M. Wierzbńska, J. Sieniawski, Effect of morphology of eutectic silicon crystals on mechanical properties and cleavage fracture toughness of AlSi5Cu1 alloy, *Journal of Achievements in Materials and Manufacturing Engineering* 14 (2006) 217-220.
- [11] L.P. Borreg, L.M. Abreu, J.M. Costa, J.M. Ferreira, Analysis of low cycle fatigue in AlMgSi aluminium alloys, *Engineering Failure Analysis* 11 (2004) 715-725.
- [12] G. Mrówka - Nowotnik, J. Sieniawski, A. Nowotnik, Tensile properties and fracture toughness of heat treated 6082 alloy, *Journal of Achievements in Materials and Manufacturing Engineering* 17 (2006) 105-108.
- [13] F.J. MacMaster, K.S. Chan, S.C. Bergsma, M.E. Kassner, Aluminium alloy 6069 part II: fracture toughness of 6061-T6 and 6069-T6, *Materials Science and Engineering A289* (2000) 54-59.
- [14] Z. Kędzierski: Role of second-phase particles in the fracture of sites with narrow plastic zone, *Metallurgy and Casting*, Volume 117, AGH Press, Kraków, 1998.
- [15] J.W. Wyrzykowski, E. Pleszakow, J. Sieniawski, *Deformation and Fracture of Metals*, WNT, Warszawa 1999.